ISSN 0020-1685, Inorganic Materials, 2023, Vol. 59, No. 8, pp. 836–841. © Pleiades Publishing, Ltd., 2023.
Russian Text © The Author(s), 2023, published in Neorganicheskie Materialy, 2023, Vol. 59, No. 8, pp. 871–877.

Defect Formation in $Gd_3Al_xGa_{5-x}O_{12}$ (x = 1–3) and $Gd_3Al_2Ga_3O_{12}$:Ce Crystals

V. M. Kasimova[a, *], **N. S. Kozlova**[a], **E. V. Zabelina**[a], **O. A. Buzanov**[b], **A. S. Bykov**[a], **E. A. Skryleva**[a], **and D. A. Spassky**[c, d]

[a] *National University of Science and Technology MISIS, Moscow, 119049 Russia*
[b] *JSC "Fomos Materials," Moscow, 107023 Russia*
[c] *Skobeltsyn Research Institute of Nuclear Physics, Moscow State University, Moscow, 119991 Russia*
[d] *Institute of Physics, University of Tartu, Tartu, 50411 Estonia*
**e-mail: kasimova.vm@misis.ru*

Received March 15, 2023; revised June 23, 2023; accepted July 3, 2023

Abstract—We present results of a detailed study of defect formation processes and their effect on the optical properties of gadolinium aluminum gallium garnet crystals with partial aluminum substitution for gallium in the cation sublattice—$Gd_3Al_1Ga_4O_{12}$ (Al : Ga = 1 : 4), $Gd_3Al_2Ga_3O_{12}$ (Al : Ga = 2 : 3), and $Gd_3Al_3Ga_2O_{12}$ (Al : Ga = 3 : 2) and cerium-doped crystals: $Gd_3Al_2Ga_3O_{12}:Ce^{3+}$ (GAGG:Ce). X-ray photoelectron spectroscopy and X-ray fluorescence analysis data demonstrate gallium deficiency relative to the stoichiometric composition in all of the crystals studied. The results obtained are used to analyze processes underlying the formation of structural growth point defects in gadolinium aluminum gallium garnet crystals. *F*-centers have been shown to be the predominant point defect species. We also have demonstrated the formation of Schottky defects and *V*-centers. The formation of additional *F*-centers in cerium-doped garnet crystals is happening. The refractive indices and attenuation coefficients of the crystals have been shown to depend on the Al : Ga ratio and doping with cerium.

Keywords: garnet, oxidation state of cerium, point defects, *F*-centers, Schottky defects, *V*-centers

DOI: 10.1134/S0020168523080058

INTRODUCTION

Crystals with the garnet structure have been known as media for laser applications since the late 1970s. A search for an optimal stoichiometric composition for new research areas led in 2011 to the synthesis of $Gd_3Al_2Ga_3O_{12}$:Ce (GAGG:Ce) crystals. Such crystals belong to a new generation of scintillators and have found application as materials of active elements in high-energy radiation detectors [1–5].

Important parameters of GAGG:Ce for subsequent application as a scintillating material are light yield and scintillation decay time [6, 7]. For this reason, to obtain crystals with commercially attractive properties, the vast majority of studies are concerned with the scintillation properties of GAGG:Ce [3, 5, 8–10] and improvement of its performance parameters [3, 10]. Structural point defects, including those due to the presence of dopants [11, 12], can have a negative effect on the optical quality of crystals and impair their scintillation and lasing characteristics [13]. The defect structure of GAGG:Ce and $Gd_3Al_xGa_{5-x}O_{12}$ (x = 1–3) has not yet been studied in sufficient detail [14–21].

The aim of this work was to study how defect formation processes are influenced by isomorphous substitutions of aluminum and gallium in the cation sublattice and doping with cerium and how they influence the optical properties of the crystals.

EXPERIMENTAL

Crystals for this investigation were grown at JSC "Fomos Materials" in iridium crucibles by the Czochralski method under an Ar + 1–2% O_2 atmosphere. The compositions of the growth charge were $Gd_{2.97}Al_2Ga_3O_{12}:Ce_{0.03}$ and $Gd_3Al_xGa_{5-x}O_{12}$ (x = 1–3). Samples for measurements had the form of plates polished on both sides.

Elemental compositions were determined using X-ray fluorescence (XRF) analysis on an ARL Perform'X spectrometer and X-ray photoelectron spectroscopy (XPS) on a PHI5500VersaProbeII (ULVAC-PHI) spectrometer at the Shared Core Facilities "Materials Science and Metallurgy," NUST MISIS.

Photoemission in the XPS method was excited by a 50-W monochromatic Al K_α ($h\nu$ = 1486.6 eV) X-ray source. The beam diameter was 200 μm. Atomic concentrations were determined from the measured integrated intensity of the O 1s, Gd 4d, Ga 3p, and Al 2p

Table 1. Cation concentrations in the crystals

Element	Atomic percent							
	calculated from the growth charge composition				XRF/XPS*			
	GAGG:Ce^{3+}	Al : Ga = 1 : 4	Al : Ga = 2 : 3	Al : Ga = 3 : 2	GAGG:Ce^{3+}	Al : Ga = 1 : 4	Al : Ga = 2 : 3	Al : Ga = 3 : 2
Gd	14.85	15.00	15.00	15.00	14.78/16.00	15.15	15.86	13.95
Al	10.00	5.00	10.00	15.00	12.98/10.80	7.12	12.89	17.08
Ga	15.00	20.00	15.00	10.00	12.08/14.40	17.73	11.25	9.01
Ce	0.15	–	–	–	0.03/–	–	–	–

* On a cleaved surface.

lines using survey scans and relative atomic sensitivity factors (PHI database).

XPS was used to study a sample of a crystal with the composition $Gd_3Al_2Ga_3O_{12}$:Ce^{3+}. To preclude surface contamination, the crystal was cleaved in air immediately before loading into the spectrometer.

Elemental compositions were determined by XRF analysis in vacuum at a pressure of 5 Pa in the chamber, using a 1.5-kW source. The data were analyzed using UniQuant software.

Optical properties were studied at the Interdepartmental Educational-Testing Laboratory of Semiconductor and Dielectric Materials "Single Crystals and Stock on their Base" of NUST MISIS. Spectral dependences of transmittance T at normal incidence of naturally polarized light and spectral and angular dependences of reflectance R of P-polarized light for evaluation of the refractive index N by the Brewster method [22] were obtained on a Cary-5000 spectrophotometer equipped with an UMA accessory. The experimental data were used to calculate the attenuation coefficient μ (cm^{-1}) with allowance for reflection and refraction in compliance with the Russian Federation State Standard GOST 3520-92, using the relation

$$\mu = -\frac{\ln\tau}{d} = -\frac{1}{d} \times \ln\left(\sqrt{\left[\frac{1}{T}\frac{8N^2}{(N-1)^4}\right]^2 + \left[\frac{N+1}{N-1}\right]^4} - \frac{1}{T}\frac{8N^2}{(N-1)^4}\right), \quad (1)$$

where τ (dimensionless) is internal transmission with allowance for reflection and d (cm) is the thickness of the sample.

RESULTS AND DISCUSSION

During high-temperature Czochralski growth of gallium-containing crystals, gallium vaporizes in the form of its oxides [13, 19], in agreement with previously reported data [23] on active vaporization of gallium oxides and oxygen above 1000°C. The melting point of GAGG:Ce is known to be 1850°C [24]. Volatility of components is determined by their partial pressure in the growth chamber. The main processes then are Ga_2O and O_2 vaporization.

This can be accompanied by defect formation processes. With allowance for electroneutrality, they can be described by quasichemical reactions represented by the following equations:

$$mO_2\uparrow \leftrightarrow 2mV_O^{++} + 4me, \quad (2)$$

$$nGa_2O\uparrow \leftrightarrow 2nV_{Ga}^{---} + nV_O^{++} + 4nh. \quad (3)$$

Here, to maintain electroneutrality, we introduce the coefficients m for O_2 and n for Ga_2O ($m > n$), which characterize the amount of vaporized components.

The processes in question lead to the presence of unoccupied lattice sites in the grown crystal, that is, to the formation of gallium vacancies (V_{Ga}^{---}) and oxygen vacancies (V_O^{++}), which, combining with free electrons (e) and holes (h), can form Schottky point defects (S), F-centers (F_c), and V-centers (V_c). For Eqs. (2) and (3) to retain integer coefficients, they are increased by three times:

$$2nV_{Ga}^{---} + 3nV_O^{++} \leftrightarrow nS, \quad (4)$$

$$6mV_O^{++} + 12me \leftrightarrow 6mF_c, \quad (5)$$

$$4nV_{Ga}^{---} + 12nh \leftrightarrow 4nV_c. \quad (6)$$

Since $m > n$, the number of F_c growth point defects exceeds that of S and V_c defects.

Using XRF analysis and XPS (of cleaved surfaces), we determined the concentrations of the major elements Gd, Al, Ga, O, and Ce in all of the crystals under study (Table 1). The results demonstrate that the elemental compositions of the crystals differ from the intended ones, with gallium deficiency in all of the crystals.

Thus, influencing the formation of structural growth point defects, such as F_c, V_c, and S, gallium oxide and oxygen vaporization processes occur in all of the $Gd_3Al_xGa_{5-x}O_{12}$ (x = 1–3) and $Gd_3Al_2Ga_3O_{12}$:Ce^{3+} crystals under study.

To assess the effect of cations substitutions and doping with cerium on defect formation processes, it is necessary to examine the distribution of elements over the corresponding sites in the garnet structure. Each unit cell in the garnet structure contains 160 atoms, of which 96 are anions forming coordination polyhedra (dodecahedra, octahedra, and tetrahedra) and 64 are cations, which are distributed over the coordination polyhedra as follows: 24 in the dodecahedra, 16 in the octahedra, and 24 in the tetrahedra [25, 26]. As shown earlier [25–27], Gd^{3+} resides predominantly on dodecahedral sites and, in addition, can be encountered in octahedra [26, 28], whereas the Al^{3+} and Ga^{3+} cations are distributed over octahedral and tetrahedral sites.

The elemental compositions determined experimentally in this study and previously reported data [25–27] on the distribution of the constituent elements over coordination polyhedra lead us to assume probabilistic defect formation models presented below.

For the formation of one unit cell corresponding to the $Gd_3Al_xGa_{5-x}O_{12}$ composition, the amounts of the constituent oxides Gd_2O_3, Al_2O_3, and Ga_2O_3 in the growth charge should correspond to the following equations:

$$12Gd_2O_3 \leftrightarrow 24Gd^{+++} + 36O^{--}, \tag{7}$$

$$4xAl_2O_3 \leftrightarrow 8xAl^{+++} + 12xO^{--}, \tag{8}$$

$$4(5-x)Ga_2O_3 \leftrightarrow 8(5-x)Ga^{+++} + 12(5-x)O^{--}. \tag{9}$$

In an ideal case, one $Gd_3Al_xGa_{5-x}O_{12}$ unit cell is formed by $24Gd^{3+}$, $8xAl^{3+}$, and $8(5-x)Ga^{3+}$. The probabilistic model takes into account that the gadolinium and aluminum are entirely, without losses, accommodated in one unit cell because they form no volatile compounds with oxygen. To model defect formation processes determined by gallium deficiency in an ideal crystal lattice, we take into account XRF results on gallium deficiency (Δ_{Ga}) per unit cell:

$$\Delta_{Ga} = \frac{w_{cr}8(5-x)}{w_{ch}}, \tag{10}$$

where w_{cr} is the gallium concentration in the grown crystal as determined by XRF analysis (Table 1) and w_{ch} is the gallium concentration in the growth charge (Table 1).

To estimate the deviation of the actual unit-cell composition from the ideal one, we introduce a specific coefficient, β, which is the ratio of the total sum of cations in an ideal unit cell (64 atoms) to the actual number of cations per unit cell:

$$\beta = \frac{64}{\Delta_{Ga} + 8x + 24}. \tag{11}$$

The closer is β to unity, the more perfect is the crystal structure and the smaller is the deviation from the stoichiometric composition.

Table 2. Specialized coefficient β for undoped $Gd_3Al_xGa_{5-x}O_{12}$ crystals

Crystal	Al : Ga = 1 : 4	Al : Ga = 2 : 3	Al : Ga = 3 : 2
x	1	2	3
Δ_{Ga}	27	17	14
β	1.08	1.12	1.03

In the case of the undoped crystals under study, the smallest deviation is observed for the crystal with an Al : Ga ratio of 3 : 2, which points to a lower density of point defects in the grown crystal (Table 2).

To dope a $Gd_3Al_2Ga_3O_{12}$ crystal with cerium, CeO_2 is added to the growth charge. Its oxidation state in the grown crystal was determined by X-ray absorption near edge structure (XANES) spectroscopy, which showed that the oxidation state of cerium in the crystals under investigation was 3+ [29].

Equations describing defect formation processes should take into account changes in the charge state of the cerium added to the growth charge:

$$2CeO_2 \leftrightarrow 2Ce^{++++} + 4O^{--}, \tag{12}$$

$$2Ce^{++++} + 2e \leftrightarrow 2Ce^{+++}. \tag{13}$$

For a change in the charge state of cerium, free electrons (e) are needed, which can be provided by reaction (14) because a large amount of oxygen vaporizes:

$$6O_O^{--} \leftrightarrow 3O_2\uparrow + 6V_O^{++} + 12e. \tag{14}$$

According to Tyagi et al. [9], Ce^{3+} can reside on dodecahedral sites. However, the ionic radius of Ce^{3+} allows it to occupy octahedral sites as well, without impairing stability of the coordination polyhedron. According to Shaskol'skaya [30], if the ratio of the ionic radius of a cation (R_c) to that of an anion (R_a) falls in the range 0.41–0.73 (in the case of octahedra), the cation can occupy the site without distorting the coordination polyhedron. The ratio R_c/R_a is 0.72, where $R_c = 1.010$ Å and $R_a = 1.40$ Å. This suggests that, upon incorporation of Ce^{3+} into octahedra, the coordination polyhedron retains its stability. In such a case, after the change in its oxidation state, cerium in the form of Ce^{3+} can force out Ga^{3+} from its octahedral site, and the released Ga^{3+} can capture electrons, with a change in its charge state to Ga^{+}, and then combine with oxygen to form Ga_2O, a volatile oxide:

$$2Ga^{+++} + 4e \leftrightarrow 2Ga^{+}, \tag{15}$$

$$2Ga^{+} + O^{--} \leftrightarrow Ga_2O\uparrow. \tag{16}$$

Free oxygen can fill an oxygen vacancy (17), and the V_O^{++} and e left can form an F_c defect (18):

$$3V_O^{++} + 3O^{--} \leftrightarrow 3O_O, \tag{17}$$

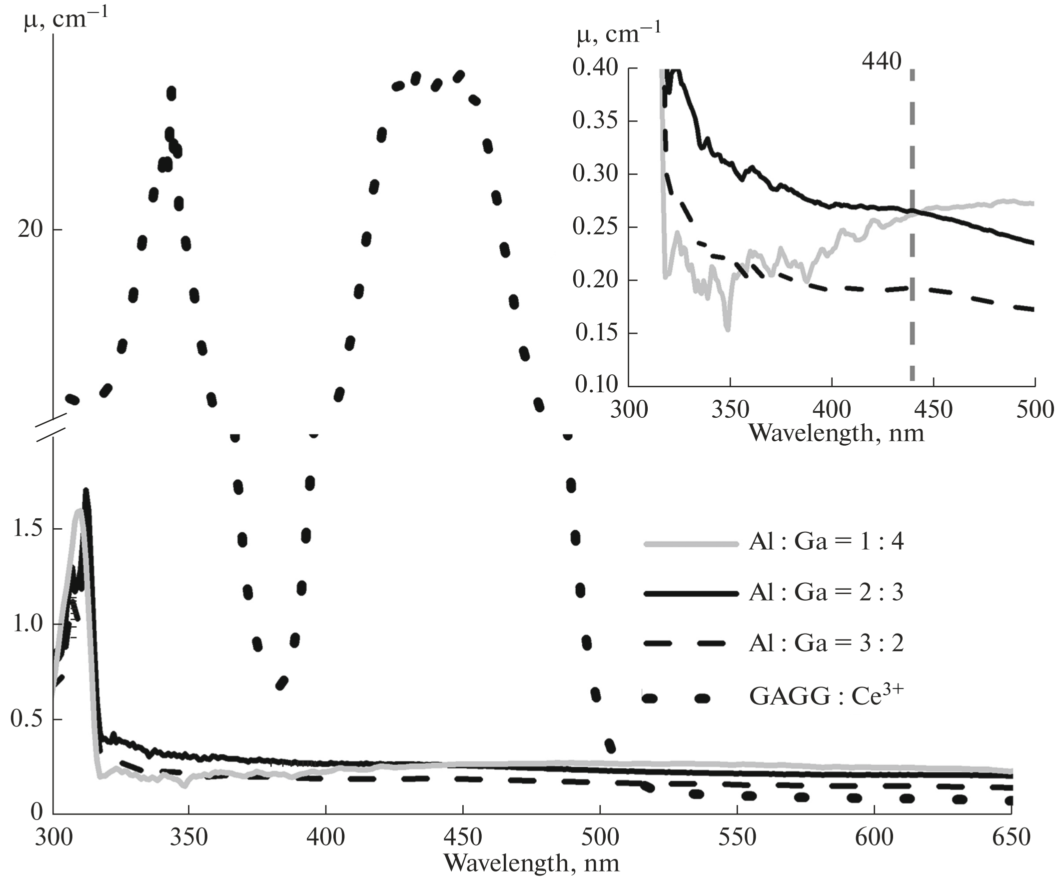

Fig. 1. Spectral dependences of the attenuation coefficient for the GAGG:Ce^{3+} and $Gd_3Al_xGa_{5-x}O_{12}$ ($x = 1$–3) crystals.

$$3V_O^{++} + 6e \leftrightarrow 3F_c. \quad (18)$$

Thus, the addition of CeO_2 to the growth charge has been shown to produce additional F_c defects in $Gd_3Al_2Ga_3O_{12}$:Ce^{3+}.

Optical properties of the crystals. In this study, we obtained light attenuation coefficients with allowance for previously measured refractive indices of the crystals under investigation [25, 29]. In previous studies [25, 29], refractive indices were observed to increase with decreasing aluminum concentration in the cation sublattice. Spectral dependences of attenuation coefficients (Fig. 1) for all of the crystals under study are nonmonotonic, with maxima in the range $\lambda = 300$–310 nm, due to intraconfigurational transitions ($4f^7$ configuration) of Gd^{3+} [9]. Attenuation in the crystal with an Al : Ga ratio of 3 : 2 is weaker than that in the other undoped crystals, which suggests a lower density of structural defects and is well consistent with results inferred from the proposed model.

Doping with cerium leads to an increase in absorption throughout the spectral range studied and causes strong, broad bands to emerge at $\lambda_{max} \sim 340$ and 440 nm. In the literature [9], the strong, broad absorption band at $\lambda_{max} \sim 440$ nm in attenuation spectra of GAGG:Ce crystals is assigned to only Ce^{3+} $4f$–$5d$ interconfigurational transitions. However, these bands are rather strong and broad, so they cannot arise from only interconfigurational transitions. As shown in the probabilistic defect formation model presented above, the incorporation of cerium into a crystal leads to the formation of additional F_c defects and their complexes, which are color centers and can produce additional bands in the range 400–500 nm. Such an effect was observed in similar mixed crystals with the garnet ($Y_3Al_5O_{12}$) structure, including those doped with cerium [32–34]. In connection with this, we conclude that the absorption band with $\lambda_{max} \sim 440$ nm is due to two mechanisms: Ce^{3+} $4f$–$5d$ interconfigurational transitions and formation of F_c structural point defects and their complexes.

CONCLUSIONS

We have studied the effects of defect formation in $Gd_3Al_xGa_{5-x}O_{12}$ ($x = 1$–3) crystals and the presence of cerium in $Gd_3Al_2Ga_3O_{12}$:Ce^{3+} on spectral dependences of attenuation coefficients. The results demonstrate that the crystal with an Al : Ga ratio of 3 : 2 has the weakest attenuation, which suggests a lower density of structural defects in this crystal.

A probabilistic defect formation model has been proposed for crystals with isomorphous substitutions of gallium and aluminum in the cation sublattice: $Gd_3Al_xGa_{5-x}O_{12}$ ($x = 1$–3) and $Gd_3Al_2Ga_3O_{12}$:Ce^{3+}:

(1) Crystal growth is accompanied by the formation of structural Schottky point defects, F_c, and V_c. The predominant defect species is F_c.

(2) The Ce^{3+}-doped crystals contain additional F_c defects in the form of complexes because cerium forces out gallium from the octahedral site.

(3) Doping with Ce^{3+} leads to the formation of a broad absorption band at $\lambda_{max} \sim 440$ nm, which is due to two mechanisms: Ce^{3+} $4f$–$5d$ interconfigurational transitions and formation of F_c structural point defects and their complexes.

ACKNOWLEDGMENTS

The optical properties of the crystals were studied at the Single Crystals and Related Raw Materials Interdepartmental Academic and Testing Laboratory of Semiconductor Materials and Dielectrics, Moscow Institute of Steel and Alloys (National University of Science and Technology).

The elemental analyses by X-ray fluorescence and X-ray photoelectron spectroscopies were carried out at the Materials Science and Metallurgy Shared Use Research and Development Center, Moscow Institute of Steel and Alloys (National University of Science and Technology).

FUNDING

The study of the optical properties of the crystals was supported by the Russian Federation Ministry of Science and Higher Education as part of the state research target no. FSME-2023-0003 for higher education institutions.

The study of the elemental composition of the crystals was supported by the Russian Federation Ministry of Science and Higher Education through the project no. 075-15-2021-696.

CONFLICT OF INTEREST

The authors declare that they have no conflicts of interest.

REFERENCES

1. Kamada, K., Yanagida, T., Endo, T., Tsutumi, K., Usuki, Y., Nikl, M., Fujimoto, Yu., and Yoshikawa, A., *2-inch size single crystal growth and scintillation properties of new scintillator; Ce:*$Gd_3Al_2Ga_3O_{12}$, *IEEE NSS/MIC,* 2011, pp. 1927–1929. https://doi.org/10.1109/NSSMIC.2011.6154387
2. Lecoq, P., Development of new scintillators for medical applications, *Nucl. Instrum. Methods Phys. Res., Sect. A,* 2016, vol. 809, p. 130. https://doi.org/10.1016/j.nima.2015.08.041
3. Alenkov, V., Buzanov, O., Dosovitskiy, G., Egorychev, V., Fedorov, A., Golutvin, A., Guz, Yu., Jacobsson, R., Korjik, M., Kozlov, D., Mechinsky, V., Schopper, A., Semennikov, A., Shatalov, P., and Shmanin, E., Irradiation studies of a multi-doped $Gd_3Al_2Ga_3O_{12}$, *Nucl. Instrum. Methods Phys. Res., Sect. A,* 2019, vol. 916, pp. 226–229. https://doi.org/10.1016/j.nima.2018.11.101
4. Martinazzoli, L., Crystal fibers for the LHCb calorimeter upgrade, *IEEE Trans. Nucl. Sci.,* 2020, vol. 67, no. 6, pp. 1003–1008. https://doi.org/10.1109/TNS.2020.2975570
5. Dilillo, G., Zampa, N., Campana, R., Fuschino, F., Pauletta, G., Rashevskaya, I., Ambrosino, F., Baruzzo, M., Cauz, D., Cirrincione, D., Citossi, M., Casa, G.D., Di Ruzza, B., Evangelista, Y., Galgóczi, G., Labanti, C., Ripa, J., Tommasino, F., Verroi, E., Fiore, F., and Vacchi, A., Space applications of GAGG:Ce scintillators: a study of afterglow emission by proton irradiation, *Nucl. Instrum. Methods Phys. Res., Sect. B,* 2022, vol. 513, pp. 33–43. https://doi.org/10.1016/j.nimb.2021.12.006
6. Lyapidevskii, V.K., *Stsintillyatsionnyi metod detektirovaniya izluchenii* (Scintillation Method of Radiation Detection), Moscow: Mosk. Inzh.-Fiz. Inst., 1981.
7. Kitaura, M., Sato, A., Kamada, K., Ohnishi, A., and Sasaki, M., Phosphorescence of Ce-doped $Gd_3Al_2Ga_3O_{12}$ crystals studied using luminescence spectroscopy, *J. Appl. Phys.,* 2014, vol. 115, no. 8, p. 083517. https://doi.org/10.1063/1.4867315
8. Kamada, K., Yanagida, T., Endo, T., Tsutumi, K., Usuki, Y., Nikl, M., Fujimoto, Yu., Fukabori, A., and Yoshikawa, A., 2 inch diameter single crystal growth and scintillation properties of Ce:$Gd_3Al_2Ga_3O_{12}$, *J. Cryst. Growth,* 2012, vol. 352, no. 1, pp. 88–90. https://doi.org/10.1016/j.jcrysgro.2011.11.085
9. Tyagi, M., Meng, F., Koschan, M., Donnald, S.B., Rothfuss, H., and Melcher, C.L., Effect of codoping on scintillation and optical properties of a Ce-doped $Gd_3Ga_3Al_2O_{12}$ scintillator, *J. Phys. D: Appl. Phys.,* 2013, vol. 46, no. 47, p. 475302. https://doi.org/10.1088/0022-3727/46/47/475302
10. Babin, V., Bohacek, P., Grigorjeva, L., Kučera, M., Nikl, M., Zazubovich, S., and Zolotarjovs, A., Effect of Mg^{2+} ions co-doping on luminescence and defects formation processes in $Gd_3(Ga,Al)_5O_{12}$:Ce single crystals, *Opt. Mater.,* 2017, vol. 66, pp. 48–58. https://doi.org/10.1016/j.optmat.2017.01.039
11. Teplyakova, N.A., Smirnov, M.V., Sidorov, N.V., and Palatnikov, M.N., Defects and some physical properties of nominally pure and zinc-doped lithium niobate crystals, *Phys. Solid State,* 2021, vol. 63, no. 8, pp. 1317–1325. https://doi.org/10.1134/S1063783421080291
12. Arsenyev, P.A. and Tkachuk, G.N., Spectroscopic properties of neodymium ions in the crystal lattice of gadolinium titanate, *Crystallogr. Rep.,* 2021, vol. 66, no. 3, pp. 486–488. https://doi.org/10.1134/S1063774521030044
13. Blistanov, A.A., *Kristally kvantovoi i nelineinoi optiki: uchebnoe posobie* (Quantum- and Nonlinear-Optical Crystals: A Learning Guide), Moscow: MISiS, 2007.
14. Fujimori, K., Kitaura, M., Taira, Y., Fujimoto, M., Zen, H., Watanabe, S., Kamada, K., Okano, Y., Katoh, M., Hosaka, M., Yamazaki, J., Hirade, T., Kobayashi, Y.,

and Ohnishi, A., Visualizing cation vacancies in Ce:$Gd_3Al_2Ga_3O_{12}$ scintillators by gamma-ray-induced positron annihilation lifetime spectroscopy, *Appl. Phys. Exp.,* 2020, vol. 13, no. 8, p. 085505. https://doi.org/10.35848/1882-0786/aba0dd

15. Meng, F., Development and improvement of cerium activated gadolinium gallium aluminum garnets scintillators for radiation detectors by codoping, *PhD Dissertation,* Knoxville, 2015.
16. Bohacek, P., Krasnikov, A., Kučera, M., Nikl, M., and Zazubovich, S., Defects creation in the undoped $Gd_3(Ga,Al)_5O_{12}$ single crystals and Ce^{3+}-doped $Gd_3(Ga,Al)_5O_{12}$ single crystals and epitaxial films under irradiation in the Gd^{3+}-related absorption bands, *Opt. Mater.,* 2019, vol. 88, pp. 601–605. https://doi.org/10.1016/j.optmat.2018.12.033
17. Yoshikawa, A., Fujimoto, Y., Yamaji, A., Kurosawa, S., Pejchal, J., Sugiyama, M., Wakahara, S., Futami, Y., Yokota, Y., Kamada, K., Yubuta, K., Shishido, T., and Nikl, M., Crystal growth and characterization of Ce:$Gd_3(Ga,Al)_5O_{12}$ single crystal using floating zone method in different O_2 partial pressure, *Opt. Mater.,* 2013, vol. 35, no. 11, pp. 1882–1886. https://doi.org/10.1016/j.optmat.2013.02.021
18. Kuzmicheva, G.M., Kozlikin, S.N., Zharikov, E.V., Kalitin, S.P., and Osiko, V.V., Point defects in gadolinium-gallium garnet, *Russ. J. Inorg. Chem.,* 1988, vol. 33, no. 9, pp. 2200–2204.
19. Zharikov, E.V., Laptev, V.V., Maier, A.A., and Osiko, V.V., Cation competition on octahedral sites of gallium garnets, *Izv. Akad. Nauk SSSR, Neorg. Mater.,* 1984, vol. 20, no. 6, pp. 857–862.
20. Komar, J., Solarz, P., Jeżowski, A., Głowacki, M., Berkowski, M., and Ryba-Romanowski, W., Investigation of intrinsic and extrinsic defects in solid solution $Gd_3(Al,Ga)_5O_{12}$ crystals grown by the Czochralski method, *J. Alloys Compd.,* 2016, vol. 688, pp. 96–103. https://doi.org/10.1016/j.jallcom.2016.07.139
21. Matkovskii, A.O., Sugak, D.Yu., Ulmanis, U.A., and Savitskii, V.G., *Tsentry okraski v redkozemel'nykh gallievykh granatakh* (Color Centers in Rare-Earth Gallium Garnets), Salaspils: LAFI, 1987.
22. Zabelina, E.V., Kozlova, N.S., Goreeva, Zh.A., and Kasimova, V.M., Multiangle spectrophotometric methods of reflection for determining refractive coefficients, *Russ. Microelectron.,* 2020, vol. 49, no. 8, pp. 617–625. https://doi.org/10.1134/S1063739720080120
23. Lamoreaux, R.H., Hildenbrand, D.L., and Brewer, L., High-temperature vaporization behavior of oxide: II. Oxides of Be, Mg, Ca, Sr, Ba, B, Al, Ga, In, Tl, Si, Ge, Sn, Pb, Zn, Cd and Hg, *J. Phys. Chem. Ref. Data,* 1987, vol. 16, no. 3, pp. 419–443. https://doi.org/10.1063/1.555799
24. *Physical and Scintillation Properties,* Furukawa Co, 2014. http://furukawa-denshi.co.jp/cgi-bin/pdfdata/20140428162950.pdf. Accessed January 6, 2022.
25. Spassky, D., Fedyunin, F., Rubtsova, E., Tarabrina, N., Morozov, V., Dzhevakov, P., Chernenko, K., Kozlova, N., Zabelina, E., Kasimova, V., and Buzanov, O., Structural, optical and luminescent properties of undoped $Gd_3Al_xGa_{5-x}O_{12}$ ($x = 0,1,2,3$) and $Gd_2YAl_2Ga_3O_{12}$ single crystals, *Opt. Mater.,* 2022, vol. 25, p. 112079. https://doi.org/10.1016/j.optmat.2022.112079
26. Li, M., Meng, M., and Chen, J., Abnormal site preference of Al and Ga in $Gd_3Al_{2.3}Ga_{2.7}O_{12}$:Ce crystals, *Phys. Status Solidi, B,* 2021, vol. 258, p. 2000603. https://doi.org/10.1002/pssb.202000603
27. Kanai, T., Satoh, M., and Miura, I., Characteristics of a nonstoichiometric $Gd_{3+\delta}(Al,Ga)_{5-\delta}O_{12}$:Ce garnet scintillator, *J. Am. Ceram. Soc.,* 2008, vol. 91, no. 2, pp. 456–462. https://doi.org/10.1111/j.1551-2916.2007.02123.x
28. Krsmanovic, R., Morozov, V.A., Lebedev, O.I., Polizzi, S., Speghini, A., Bettinelli, M., and Van Tendeloo, G., Structural and luminescence investigation on gadolinium gallium garnet nanocrystalline powders prepared by solution combustion synthesis, *Nanotecnology,* 2007, vol. 18, p. 325604. https://doi.org/10.1088/0957-4484/18/32/325604
29. Kasimova, V.M., Kozlova, N.S., Buzanov, O.A., Zabelina, E.V., Targonskii, A.V., and Rogachev, A.V., Effect of partial substitution of aluminium for gallium on the properties of gadolinium aluminum gallium garnet single crystals, *Inorg. Mater.,* 2022, vol. 58, no. 3, pp. 288–294. https://doi.org/10.1134/S0020168522030062
30. Shaskol'skaya, M.P., *Kristallografiya* (Crystallography), Moscow: Vysshaya Shkols, 1984.
31. Shannon, R.D., Revised effective ionic radii and systematic studies of interatomic distances in halides and chalcogenides, *Acta Crystallogr., Sect. A: Cryst. Phys., Diffr., Theor. Gen. Crystallogr.,* 1976, vol. 32, no. 5, pp. 751–767. https://doi.org/10.1107/S0567739476001551
32. Pujats, A. and Springis, M., The *F*-type centers in YAG crystals, *OPA,* 2001, vol. 155, nos. 1–4, pp. 65–69. https://doi.org/10.1080/10420150108214094
33. Polisadova, E.F., Han Tao, Oleshko, V.I., Valiev, D.T., Vaganov, V.A., Sonshi, Z., and Burachenko, A.G., Effect of cerium concentration on luminescence properties of $Y_3Al_5O_{12}$:Ce under ultraviolet excitation, *Fundam. Issled.,* 2017, vol. 12, no. 1, pp. 103–109. https://doi.org/10.17513/fr.41987
34. Zorenko, Yu.V., Savchin, V.P., Gorbenko, V.I., Voznyak, T.I., Zorenko, T.E., Puzikov, V.M., Dan'ko, A.Ya., and Nizhankovskii, S.V., Luminescence and scintillation properties of $Y_3Al_5O_{12}$:Ce single crystals and single-crystal films, *Phys. Solid State,* 2011, vol. 53, no. 8, pp. 1620–1625. https://doi.org/10.1134/S1063783411080348